



Adsorption of methylene blue from aqueous solutions by cellulose and nanofiber cellulose and its electrochemical regeneration

Mohammad Hadi Mehdinejad^a, Nezamaddin Mengelizadeh^{b,c,*}, Abotaleb Bay^d, Hamidreza Pourzamani^{e,f}, Yaghoub Hajizadeh^{e,f}, Nouredin Niknam^g, Amir Hossein Moradi^h, Majid Hashemiⁱ, Hamed Mohammadi^j

^aEnvironmental Health Research Center, School of Public Health, Golestan University of Medical Sciences, Gorgan, Iran, email: hmnejad@yahoo.com (M.H. Mehdinejad)

^bEnvironment Research Committee, Isfahan University of Medical Sciences, Isfahan, Iran, Tel. +9392312472; email: nezam_m2008@yahoo.com (N. Mengelizadeh)

^cStudent Research Committee and Department of Environmental Health Engineering, School of Health, Isfahan University of Medical Sciences, Isfahan, Iran

^dDepartment of Environmental Health Engineering, School of Public Health, Shahid Beheshti University of Medical Sciences, Tehran, Iran, email: abotaleb_bay@yahoo.com (A. Bay)

^eEnvironment Research Center, Research Institute for Primordial Prevention of Non-communicable disease, Isfahan University of Medical Sciences, Isfahan, Iran, emails: pourzamani@hlth.mui.ac.ir (H. Pourzamani), yaghoub_hajizadeh@yahoo.com (Y. Hajizadeh)

^fDepartment of Environmental Health Engineering, School of Health, Isfahan University of Medical Sciences, Isfahan, Iran

^gSchool of Management and Medical Information, Iran University of Medical Sciences, Tehran, Iran, email: noureddin.niknam@yahoo.com (N. Niknam)

^hDepartment of Occupational Health & Safety, School of Health, Isfahan University of Medical Sciences, Isfahan, Iran, email: amir.h1990m@yahoo.com (A.H. Moradi)

ⁱEnvironmental Health Engineering, School of Health, Kerman University of Medical Sciences, Kerman, Iran, email: mhashemi120@gmail.com (M. Hashemi)

^jStudent Research Committee and Department of Environmental Health Engineering, School of Health, Isfahan University of Medical Sciences, Isfahan, Iran, email: hamed.mohamadi36@gmail.com (H. Mohammadi)

Received 6 May 2017; Accepted 18 March 2018

ABSTRACT

This study was conducted to evaluate the potential of the bleached bagasse, cellulose, and nanofiber cellulose to remove methylene blue (MB) from aqueous solution. The morphology of adsorbents surface and their functional groups were examined by using scanning electron microscope and Fourier transform infrared spectroscopy techniques, respectively. In a batch mode study at 25°C temperature, the effects of initial dye concentration, contact time, adsorbent dose, and solution pH on adsorption performance were investigated. The results showed that the percent of MB removal increases by increasing pH and also by increasing sorbent dosage and decreasing initial dye concentration. The adsorption kinetics and equilibrium data were in good agreement with the pseudo-second-order kinetic model and Freundlich adsorption isotherm, respectively. The removal of MB was better and more effective with cellulose and cellulose nanofiber as compared with the bleached bagasse. The regeneration of cellulose and nanofiber cellulose loaded with MB was investigated using electrochemical method under different operating conditions. The results showed that the electrochemical process efficiency is more than 60% for regeneration adsorbents.

Keywords: Adsorption; Cellulose; Electrochemical; Nanofiber cellulose; Methylene blue

* Corresponding author.

1. Introduction

Effluents from textile industry and some similar industries mainly contain color, dissolved solids, heavy metals, and high amounts of surfactants [1]. The discharge of dye into natural streams has caused many major problems, such as increasing the toxicity and chemical oxygen demand of the effluent and reducing light penetration, which has an adverse effect on photosynthetic phenomena [2,3]. Methylene blue (MB) is the most commonly used material for dyeing cotton, wood, paper, temporary hair colorant, and coating for paper stock. Although MB is not so dangerous, it can cause some harmful effects. Long-term exposure to MB will cause increased heart rate, Heinz body formation, vomiting, cyanosis, tissue necrosis, and methemoglobinemia in humans [4,5]. Therefore, the removal of the MB dye from aqueous solutions is important.

The conventional methods for treating water and wastewaters containing dyes are electrochemical degradation [6], chemical coagulation/flocculation [7], ultrafiltration [8], advanced oxidation processes [9], and adsorption [5]. Among these methods, adsorption on activated carbon is the most commonly used method in wastewater treatment because of its simple operation and high efficiency [10]. However, its use is restricted due to its high production costs and difficulty of regeneration [11,12]. Recently, various adsorbents derived from agricultural wastes or natural materials have been intensively investigated for dye removal from aqueous solutions [5]. Some of these natural low-cost adsorbents are rice biomass [13], natural palygorskite [14], bentonite [15], coal ash [16], montmorillonite clay [17], chitin [18], cellulose [19,20], banana leaves [21], canola residues [22], and *Platanus orientalis* leaf powder [23]. Among these natural low-cost adsorbents, cellulose is the most abundant natural polymer in nature, which can be obtained from agricultural wastes such as bagasse [24].

Sugarcane residue after sugar extraction is one of the most available agricultural wastes in some developing countries like Iran. Approximately, 4.3 million tons of sugarcane bagasses are produced annually in Iran, and the production is mainly centered in the southwestern province of Khuzestan. High levels of this waste are burned due to lack of necessary infrastructure and industrial use of this material. Sugarcane wastes contain compounds such as cellulose (40%–50%), lignin (18%–24%), and hemicellulose (25%–35%). Therefore, this research was conducted to study the use of bagasse and its derivatives as adsorbents for the removal of MB dye. The effect of pH, adsorbent dose, initial dye concentration, and contact time was also studied. In addition, the regeneration performance of cellulose and nanofiber cellulose-loaded MB dye was investigated using electrochemical process with Ti/TiO₂-RuO₂ and graphite felt electrodes under current density of 25 mA/cm² and elapsed time of 3 h.

2. Materials and methods

2.1. Materials

MB (Table 1) was obtained from Sigma-Aldrich. Sodium chlorite, acetic acid, sodium sulfite, and sodium hydroxide were purchased from Merck Company and were used without further purification.

2.2. Extraction of cellulose from bagasse

Sugarcane bagasse was collected from sugar factory in Khuzestan province, Iran. It was washed with some amounts of distilled water to remove sugars and ash components and was air dried to constant weight. The air-dried bagasse was screened using a 60-mesh sieve. The dried and ground bagasse was boiled with 0.7% (w/v) sodium chlorite for 5 h, filtered out, and dried in an oven at 55°C for 24 h. The dried materials were then boiled with 250 mL of 5% (w/v) sodium sulfite solution and 250 mL of 17.5% (w/v) sodium hydroxide for 5 h [25]. After chemical pretreatment, the cellulose fibers were soaked in distilled water (concentration: ~0.5% in mass). About 100 mL of the solution containing cellulose fibers was then placed in a common ultrasonic generator (JY98-IIID, Ningbo Scientz Biotechnology Co., Ltd., China) of 30 kHz for 30 min to isolate the cellulose with submicron size [26]. The sample was dried and kept at 25°C temperature for comparison with cellulose nanofiber purchased from Iranian companies in the process of adsorption of MB. In this study, the cellulose extracted from the bagasse was prepared as shown in Fig. 1. Scanning electron microscope (SEM) micrograph and Fourier transform infrared spectroscopy (FTIR) spectra of cellulose nanofiber are shown in Fig. 2.

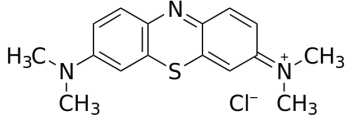
2.3. Characterization of adsorbents

Morphology and structure of the bleached bagasse, alkali-treated bagasse, and cellulose were characterized by SEM (Philips XI30, Netherlands). Functional groups of biopolymers were analyzed using a Perkin-Elmer-283B FTIR spectrometer within the wave range of 400–4,000 cm⁻¹. X-ray fluorescence spectrometer, Bruker AXS S4 Pioneer (X-ray tube anode: Cu, wavelength: 1.5406 Å [Cu Kα], filter: Ni), was used for the chemical composition analysis. The points of zero charge (PZC) adsorbents were determined by using the method of Hu et al. [27].

2.4. Adsorption studies

Adsorption studies were performed by shaking 100 mg of adsorbent with 100 mL of dye solution of known concentration and pH in a 250 mL Erlenmeyer flask. The Erlenmeyer flasks were then shaken at a constant speed of 250 rpm on a shaker (orbital shaker Model KS260B, IKA Company,

Table 1
Properties and characteristics of MB

Generic name	Methylene blue
Synonyms	3,7 bis(dimethylamino) phenazathionium chloride tetramethylthionine chloride
Formula	C ₁₆ H ₁₈ ClN ₃ S ₃ H ₂ O
Molecular weight	319.85 g/mol
Chemical structure	

Germany) at 25°C temperature. After shaking the flasks for 1 h, biopolymers were separated by centrifugation. In each experiment, the effect of a parameter on adsorption MB was studied by keeping other parameters.

Before and after each experiment, MB concentration was determined by using the UV spectrophotometer (Shimadzu, Japan) at 668 nm. All the experiments were repeated three times and only the mean values were reported.

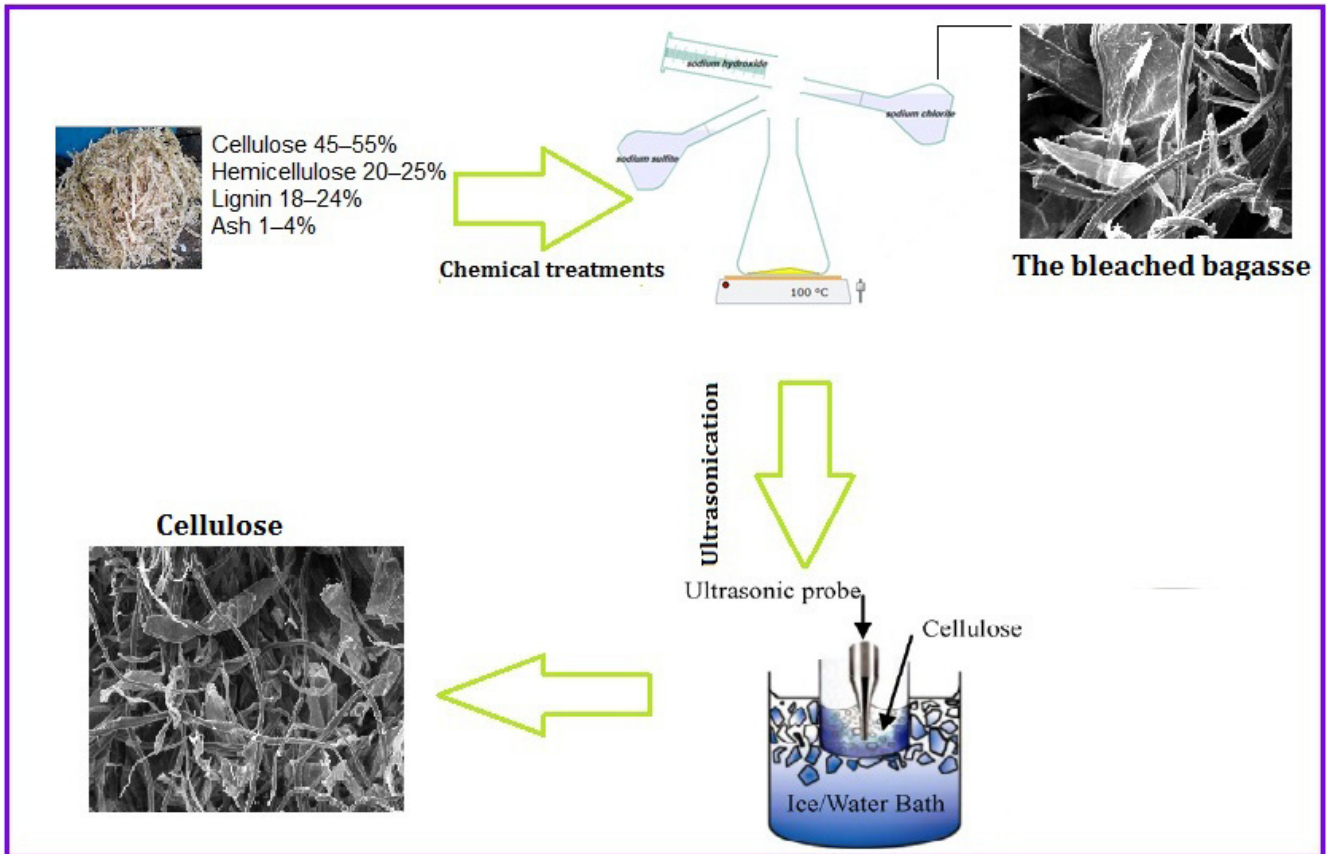


Fig. 1. Procedure for extraction of cellulose from bagasse.

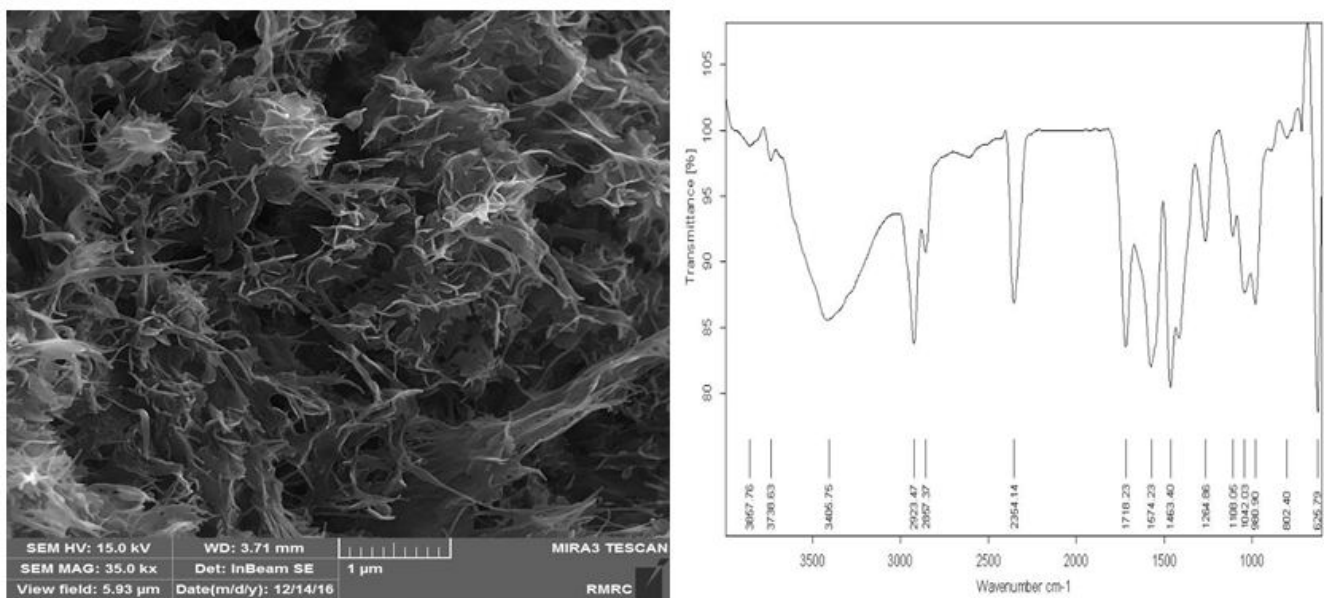


Fig. 2. SEM and FTIR spectra of cellulose nanofiber.

The pH of the solution was measured at the beginning (pH_{in}) and at the end (pH_{out}) of each experiment. The pH_{in} was adjusted using 0.01 M HCl and 0.01 M NaOH and determined by using a pH meter (CyberscanpH1500, Thermo Fisher Scientific Inc, Netherlands). The amount of adsorbed MB on adsorbent (q_e , mg/g) and percent removal (%R) was calculated as follows:

$$q_e = \frac{(C_0 - C_e)V}{m} \quad (1)$$

$$\%R = \frac{(C_0 - C_e)}{C_0} \times 100 \quad (2)$$

where C_0 and C_e (mg/L) are the MB concentrations at the input and output of each experiment, V (L) is the initial solution volume, and m (g) is the adsorbent weight.

2.5. Adsorption isotherms

Adsorption isotherms of biopolymers were studied at different initial concentrations of MB dye using ISOtherm Flitting Tool (ISOFIT) software.

ISOFIT is a software program that fits isotherm parameters to experimental data by minimizing the weighted sum of squared error objective function. ISOFIT supports a number of isotherms, including (1) Brunauer–Emmett–Teller (BET), (2) Freundlich, (3) Freundlich with linear partitioning (F-P), (4) generalized Langmuir–Freundlich (GLF), (5) Langmuir, (6) Langmuir with linear partitioning (L-P), (7) Linear, (8) Polanyi, (9) Polanyi with linear partitioning (P-P), and (10) Toth.

2.6. Adsorption kinetics

Pseudo-first order, pseudo-second order, and Elovich were used to test the experimental data to evaluate the kinetic mechanisms of adsorption process, which includes mass transfer and chemical reaction, and all the equations are listed in Table 2.

2.7. Desorption studies

Regeneration experiments of cellulose and nanofiber cellulose were performed in an electrochemical batch reactor (Fig. 3) containing Ti/TiO₂-RuO₂ (anode) and graphite felt (cathode) electrodes as shown in Fig. 3. Both anode and

cathode have an area of 50 cm², and there was a fixed distance of 1 cm between anode and cathode in these experiments. The characteristics of anode and cathode are as shown in Figs 4 and 5, and Table 3. Before the regeneration process, MB adsorption was performed under pH 7, adsorbent dose of 1,000 mg/L, MB concentration of 150 mg/L, and contact time of 120 min. One gram of saturated adsorbents was then put into the electrochemical cell; this contained 400 mL of synthetic solution with 3 g/L NaCl. Electrolysis was stopped after 3 h elapsed. After regeneration of adsorbents, its adsorption capacity was examined using adsorption experiments in 120 min. The influence of different operating parameters on the regeneration of adsorbents was studied by varying one parameter and keeping the others constant.

3. Results and discussion

3.1. Characterization of adsorbents

FTIR spectroscopy has been widely used to identify the presence of functional groups on biopolymers; also, it presents a relatively easy method of obtaining direct information on chemical changes that occur during various chemical treatments [25]. In the FTIR analysis, the spectra of bagasse and its derivatives are as shown in Fig. 6.

FTIR spectra of the bagasse and its derivatives have presented a broad band in the region of 3,000–3,500 cm⁻¹ that indicates the O–H stretching vibrations of the OH groups in cellulose molecules [25,26]. Moreover, peaks at 2,903.14 cm⁻¹ of all the samples are related to C–H stretching vibration [26]. Vibration peak detected at around 1,640 cm⁻¹ in all the samples was assigned to C=C stretching band and adsorbed

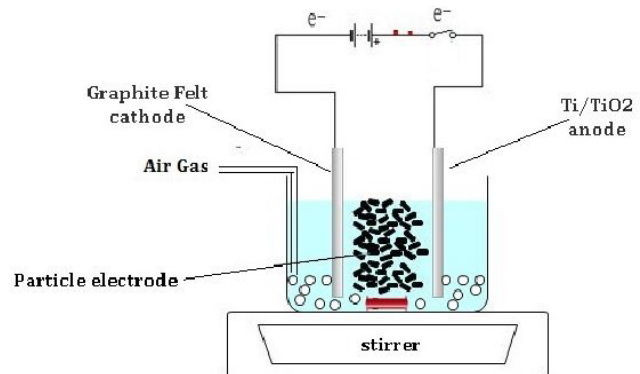


Fig. 3. Schematic diagram of the electrochemical reactor.

Table 2
Kinetic models

Kinetic model	Linear form	Eq.	Plots	Ref.
Pseudo-first order	$\log(q_e - q_t) = \log q_e - k_1 t$	(3)	$\log(q_e - q_t)$ vs. t	[27]
Pseudo-second order	$\frac{t}{q_t} = \left[\frac{1}{k_2 q_e^2} \right] + \frac{1}{q_e} t$	(4)	$\frac{t}{q_t}$ vs. t	
Elovich	$q_t = \frac{1}{\beta} \ln(\alpha\beta) + \frac{1}{\beta} \ln t$	(5)	q_t vs. $\ln t$	

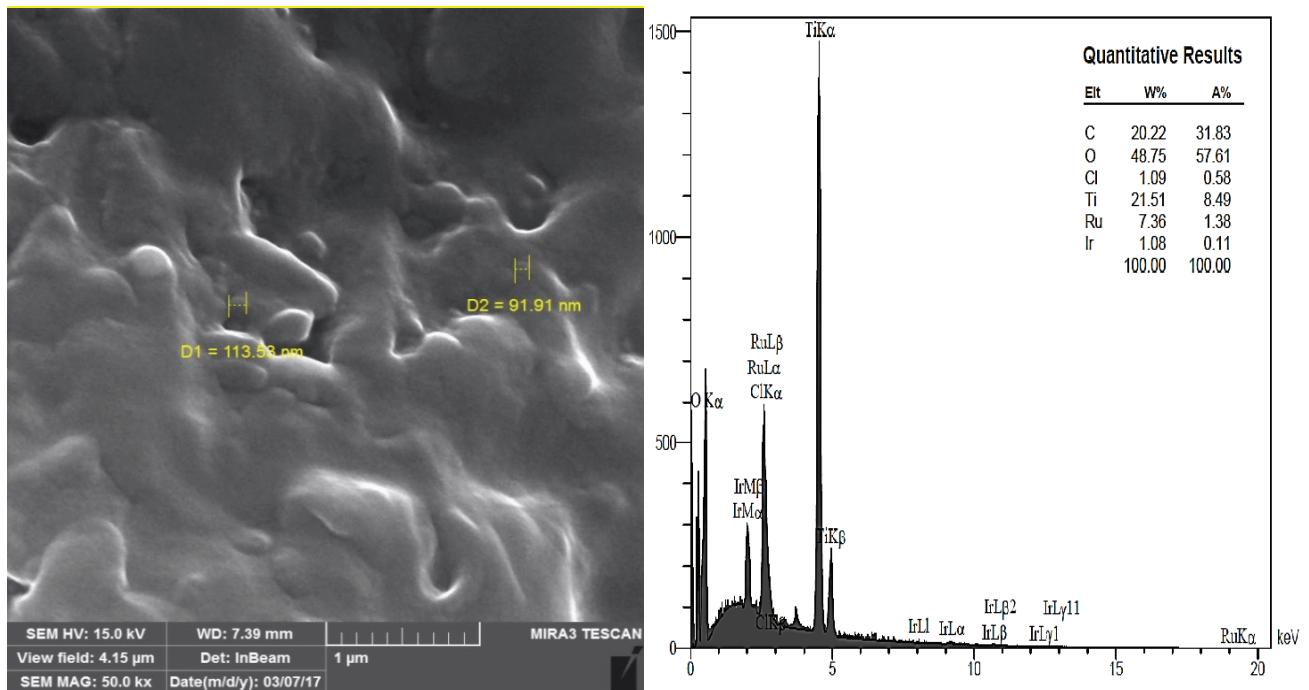


Fig. 4. SEM image and energy-dispersive X-ray spectroscopy spectrum of Ti/TiO₂-RuO₂.

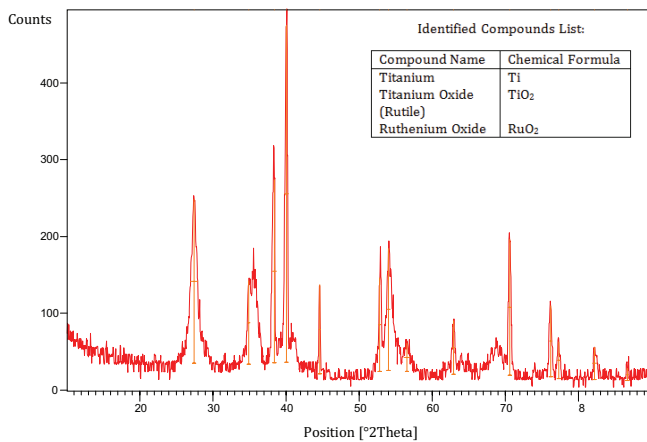


Fig. 5. X-ray diffraction analysis of Ti/TiO₂-RuO₂.

Table 3
Characteristics of graphite felt

Thickness, mm	3.2
Bulk density, g/cm ³	0.08
Areal weight, g/m ²	245
Electrical resistivity (through plane)	Less than 3 ohm mm
Carbon content (%)	99% minimum
Ash content	Less than 0.2%

water molecules [25,28]. Spectrum from 1,300 to 1,500 cm⁻¹ was attributed to the C–H bending bands [29]. C–O–C pyranose ring skeletal vibration occurs in region of 1,014–1,075 cm⁻¹ [30]. In this region, the most important absorption band continually increases on untreated sugarcane bagasse,

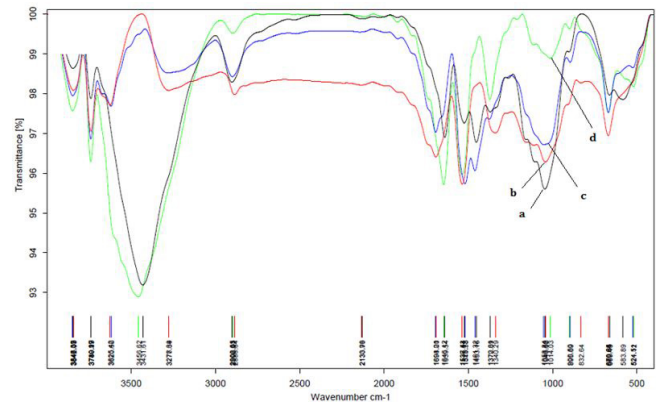


Fig. 6. FTIR spectra of (a) untreated sugarcane bagasse, (b) the bleached bagasse, (c) alkali-treated bagasse, and (d) cellulose.

the bleached bagasse, alkali-treated bagasse, and cellulose, respectively. Peak at 895–900 cm⁻¹ is connected with glycosidic C₁–H deformation, a ring vibration and –O–H bending [31]. Moreover, some peaks in the 600–800 cm⁻¹ region are related to the aromatic ring C–H out of plane bending vibration found in Figs. 6(a)–(c) and those not seen or that appeared weaker for cellulose due to the removal of lignin using the chemical and ultrasonic treatments [32].

X-ray diffraction patterns of the bleached bagasse, alkali-treated bagasse, and cellulose are as shown in Fig. 7. As shown in Fig. 7, three fibers had diffraction peaks around 2θ = 22° and 2θ = 14°, representing the presence of crystalline and amorphous cellulose structure, respectively. Crystallinity was determined by Eq. (6) using the highest peak of the amorphous (*I*_{am}) and crystalline peak (*I*₀₀₂) background region located approximately 2θ around 14° and 22.5°, respectively. By following this equation, the crystallinity index of

the bleached bagasse was approximately 60%, while that of alkali-treated bagasse and cellulose fibers were estimated to be 66.6% and 75%, respectively. When the results were compared, cellulose from bagasse obtained in this study exhibited similar crystallinity with cellulose produced by Lani et al. [33].

$$\% \text{ Crystallinity} = \frac{I_{002} - I_{\text{am}}}{I_{002}} \times 100 \quad (6)$$

Figs. 8(a)–(c) show the representative SEM images of the bleached bagasse, alkali-treated bagasse, and cellulose structure, and apparently, it reveals the effect of the chemical treatment on the shape and size of fibers. Moreover, as shown in Fig. 8(c), cellulose is typically produced from the chemical treatment of bagasse fibers. The isoelectric point was determined via zeta potential measurements for all the samples.

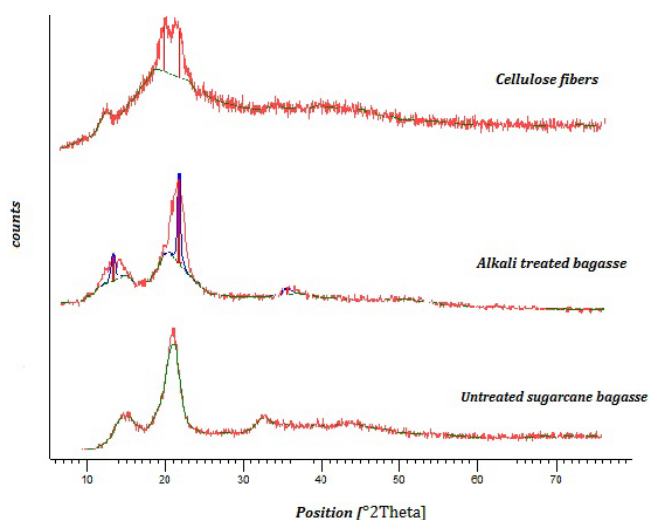


Fig. 7. X-ray diffraction patterns for (a) the bleached bagasse, (b) alkali-treated bagasse, and (c) cellulose.

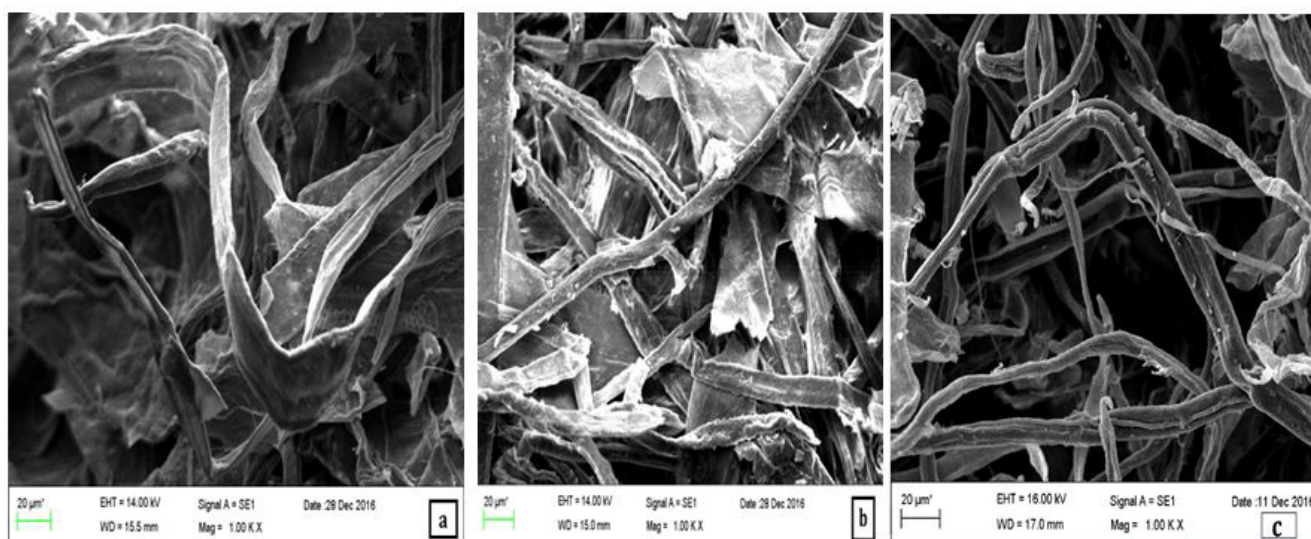


Fig. 8. SEM micrograph of (a) the bleached bagasse, (b) alkali-treated bagasse, and (c) cellulose.

The isoelectric point for the bleached bagasse, alkali-treated bagasse, and cellulose was around pH 3. Previous reports show that the PZC of cellulose and cellulosic fibers is lower than 4 [28,34,35].

3.2. Influence of physico-chemical parameters on MB dye removal efficiency

3.2.1. Effect of initial solution pH

The removal of dye from aqueous solutions through adsorption depends on the solution pH, because the acidity and alkalinity of the solution affect the ionization of the anionic and cationic dye and concentration of the counter H^+ and OH^- ions of the surface groups. The knowledge of an optimum pH is important to maximize the removal of MB dye by using the adsorbents. Changes observed in the adsorption of MB dye using the adsorbents as a function of solution pH are as shown in Fig. 9. It has been shown that the MB dye removal efficiencies by the bleached bagasse, cellulose, and nanofiber cellulose increase with increase in pH in the range of 2–10. This result may be due to a change in surface charge of both the dyes' molecules and functional groups of adsorbents.

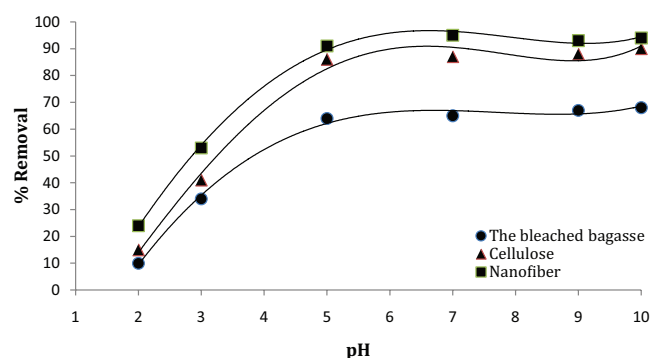


Fig. 9. pH effect on MB removal by the bleached bagasse, cellulose, and nanofiber cellulose (MB = 50 mg/L, adsorbent dose = 1 g/L, time = 60 min).

For adsorbents possessing functional groups, such as $-\text{COO}^-$ and $-\text{OSO}_3^-$, the negative surface charge decreased as pH approached the pK_a of the functional groups [36]. While at higher $\text{pH} > \text{PZC}$, there is a net negative charge on the adsorbents surface and the ionic state of functional groups such as carboxyl and hydroxyl. As a result, the adsorbent MB dye interactions become increasingly important for larger pH values [37]. This result is similar to the finding of Low et al. [38], who reported that the sorption of the MB onto lignocellulosic materials increased as the pH increased from 2 to 10. Chan et al. [39] also reported that the sorption of MB on cellulose nanofibrils gradually increased as the pH increased from 3 to 9.

In addition, as shown in Fig. 9, both cellulose and nanofiber cellulose have very high removal efficiencies and they reach 15.0%–90% for cellulose and 24%–94% for nanofiber cellulose, respectively. The dye removal efficiency by the bleached bagasse is only 10%–68% in the studied pH range. The results also showed that the adsorption of MB dye onto the nanofiber cellulose is higher than the cellulose and bleached bagasse. It has been shown that the increase of sorption capacity of nanofiber cellulose should be ascribed to the additional carboxyl groups and high surface area. A similar result was reported for the adsorption of MB onto nanocellulose hybrid [40] and carboxylate-functionalized cellulose nanocrystals [41].

3.2.2. Effect of adsorbent dosage

The effect of adsorbent dosage on MB dye removal was analyzed by varying the dosage of the bleached bagasse, cellulose, and nanofiber cellulose and the results are as shown in Fig. 10. It can be observed from this figure that the dye-removal efficiency increases with increase in adsorbent dose from 0.1 to 1 g/L for all the adsorbents. This behavior shows that when the amount of adsorbent increases, the amount of available sorption sites increases. Batmaz et al. [42] obtained the same results and showed that the amount of dye removed increased from 77% to 92% as the adsorbent dose increased from 4 to 25 mg/mL. Raghuvanshi et al. [43] also showed that the adsorption of MB dye on bagasse increased sharply when the initial adsorbent concentration is higher. Increase in adsorption with adsorbent dose can be attributed to increased adsorbent surface area and availability of more adsorption sites.

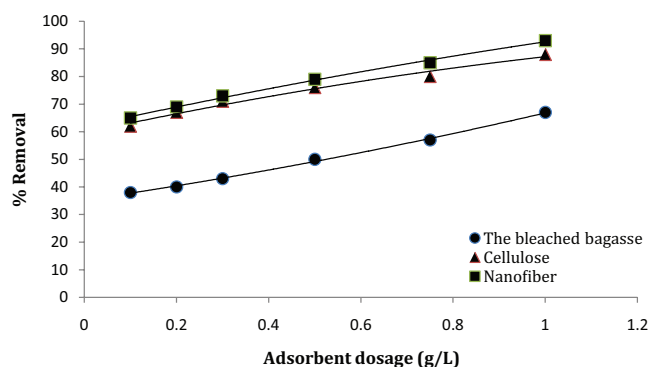


Fig. 10. Dosage adsorbent effect on MB removal by the bleached bagasse, cellulose, and nanofiber cellulose (initial pH = 7, MB = 50 mg/L, time = 60 min).

Fig. 10 shows the comparison of sorption efficiency of the bleached bagasse, cellulose, and nanofiber cellulose. Nanofiber cellulose shows maximum removal efficiency at minimum dose (0.8 g) as compared with maximum concentration of the cellulose and the bleached bagasse. The enhanced sorption efficiency of nanofiber cellulose can be ascribed to the removal of the non-cellulosic amorphous constituents, which promote the availability of large number of $-\text{OH}$ free groups on the nanocellulose chains. The findings are in conformity with the observations of Kardam et al. [44].

3.2.3. Effect of initial dye concentration

Fig. 11 shows the percentage of the MB removal using the bleached bagasse, cellulose, and nanofiber cellulose. The various dye concentrations ranging from 25 to 150 mg/L were used in this experiment at 25°C temperature using 1 g/L adsorbent dosage at pH 7. As shown in Fig. 11, removal of MB decreased by increasing the initial dye concentration. For example, at initial pH solution of 7, MB removal dropped from 93.5% to 69.11% using nanofiber cellulose when the initial dye concentration varied from 25 to 150 mg/L. This observation can be explained on the basis of lack of sufficient surface area to accommodate much dye available in the solution. At lower concentrations, all dye ions present in solution could interact with the binding sites and thus making the percentage of removal higher than those at higher dye ion concentrations. Similar result was found for the methyl red removal using untreated sugarcane bagasse, where the percentage of dye removal decreased from 70% to 30% as dye concentration increased from 50 to 250 mg/L [45]. Zhang et al. [46] also reported that Rhodamine B (RhB) removal by bagasse decreased from 99.1% to 87.1% with increase in initial RhB concentration from 100 to 500 mg/L.

3.2.4. Effect of contact time and adsorption kinetics

Fig. 12 shows the effects of contact time on the adsorption of MB onto the bleached bagasse, cellulose, and nanofiber cellulose. MB solution with an initial concentration of 50 mg/L and pH value of 7.0 was used to study the adsorption kinetics. As shown in this figure, the initial adsorption is rapid for all the three samples, where maximum removal efficiencies of the adsorption take place within 60 min. This rapid increase of

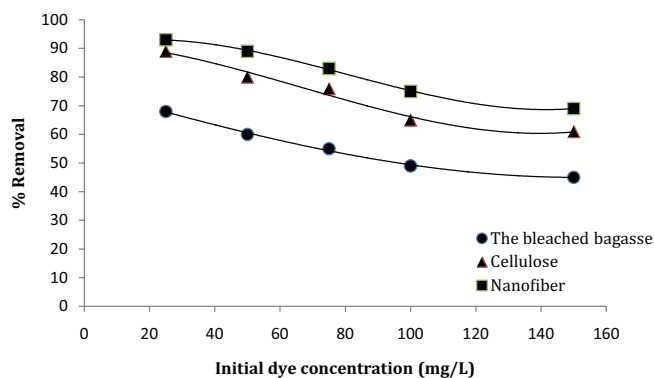


Fig. 11. Initial dye concentration effect on MB removal by the bleached bagasse, cellulose, and nanofiber cellulose (initial pH = 7, adsorbent dose = 1 g/L, time = 60 min).

adsorption can be attributed to the strong electrostatic interaction between the negatively charged surface of adsorbent and the cationic dye due to increase in the number of vacant sites available at the initial contact time [14]. Further increase in contact time from 60 to 120 min increased the efficiency of adsorption very slowly, due to the decrease of adsorptive sites for the residual dye molecules in the solution [47]. Similar results were also obtained by Liu et al. [48] for the adsorption of MB using Attapulgitte/Bentonite complex. Moreover, sorption studies in literature reveal that the uptake of adsorbate species is fast at the initial stages of the contact period, and afterwards, it becomes slower when is near to equilibrium [49].

To investigate the mechanism of sorption and its potential rate-controlling steps, which include chemical reaction processes and mass transport, kinetic models have been exploited to analyze the experimental data. In addition, information on the kinetics of dye uptake is required to select the optimum condition for full-scale batch pollutant removal processes. The kinetics of MB sorption onto adsorbents was assessed by using different kinetic models and corresponding parameters calculated are shown in Table 4. This table shows the correlation coefficients (R^2) for the pseudo-second-order kinetic model to be higher than pseudo-first-order and Elovich kinetic models. The q_e values calculated from pseudo-second-order kinetic model are also close to the experimental data (q_{exp}). Similar results were observed for the adsorption of MB from aqueous solution on various adsorbent [49–52].

3.2.5. Isotherm study

The adsorption equilibrium data of MB on the bleached bagasse, cellulose, and nanofiber cellulose adsorbents were fitted by using several well-known isotherm models to assess their efficacies. In this study, ISOFIT was applied to

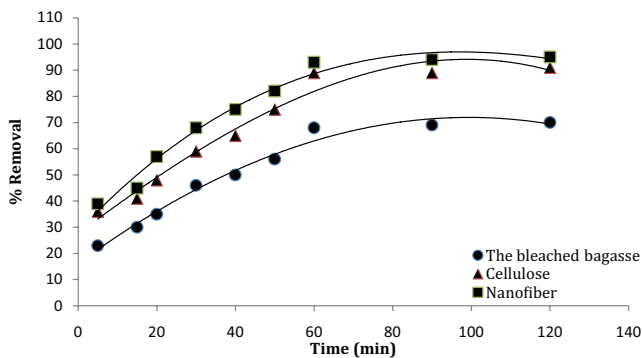


Fig. 12. Effect of contact time on MB removal by the bleached bagasse, cellulose, and nanofiber cellulose (initial pH = 7, MB = 50 mg/L, adsorbent dose = 1 g/L).

Table 4
Kinetics adsorption rate constants, calculated $q_{e,cal}$ and experimental q_e values of MB dye on the adsorbents

Adsorbent	$q_{e,exp}$ (mg/g)	First-order kinetic model			Second-order kinetic model			Elovich model		
		k_1	$q_{e,cal}$ (mg/g)	R^2	k_2	$q_{e,cal}$ (mg/g)	R^2	α	β	R^2
The bleached bagasse	17	0.029	14.1	0.945	0.0033	17.88	0.984	7.14	0.297	0.910
Cellulose	22.25	0.029	17.45	0.938	0.0031	22.47	0.955	6.60	0.240	0.856
Nanofiber cellulose	23.25	0.036	18.314	0.955	0.0029	25.06	0.978	6.39	0.207	0.894

involving the adsorption of MB with initial concentration of 25–150 mg/L (25, 50, 75, 100, and 150 mg/L) by the bleached bagasse, cellulose, and nanofiber cellulose. Fig. 13 shows the plots of the fitted isotherms for MB adsorption by adsorbents (organized into visually indistinguishable groups) along with the observed data points. Table 5 shows the corrected Akaike information criterion (AICc) values of isotherm study. The results show that the Freundlich isotherm expression provided the best fit of the sorption data based on its relatively low value of AICc. Table 6 also summarizes the resulting parameters estimated for the Freundlich isotherm. San Keskin et al. [53] studied the adsorption isotherm of reactive dye and hexavalent chromium from aqueous solutions onto reusable bacteria attached to electrospun nanofibrous web by ISOFIT software; their study showed that the Toth-generalized isotherm expression provides the best fit of reactive dye adsorption by reusable bacteria; Langmuir and GLF models isotherm expression provides the best fit of hexavalent chromium adsorption by reusable bacteria. The adsorption process of dyes on cellulosic waste studied by Namasivayam et al. [54] shows the adsorption equilibrium isotherms fitted by both the Langmuir and Freundlich isotherms. Nourmoradi et al. [55] used ISOFIT for the adsorption of humic acid by surfactant-modified nanozeolite (SMNZ). Their results show that the L-P isotherms provide the best fit of the sorption data for humic acid by SMNZ.

The comparisons of maximum adsorption capacities of the adsorbents obtained in this study with various adsorbents previously studied for the adsorption of MB are shown in Table 7. As shown, the MB adsorption capacity of cellulose nanofiber is 119.04 mg/g at 298 K, which is higher than that of the bleached bagasse and cellulose studied. Furthermore, this value is also much higher than other adsorbents obtained from natural materials such as agricultural and industrial solid wastes. This comparison suggests that nanocellulose may be an effective adsorbent for MB removal from contaminated water.

3.3. Electrochemical regeneration of adsorbents

It is important to test the repeated availability performance of MB sorption onto adsorbents to reduce the cost of replacement of adsorbents in aqueous solutions treatment before its practical use for environmental protection applications. Therefore, the influence of electrolyte concentration, current intensity, and reaction time on the electrochemical regeneration adsorbents was examined in this study. The result in Fig. 14 shows that the regeneration efficiency of cellulose and nanofiber cellulose increases with increase in the regeneration current intensity, electrolyte concentration, and time. The increase in adsorbents regeneration is related

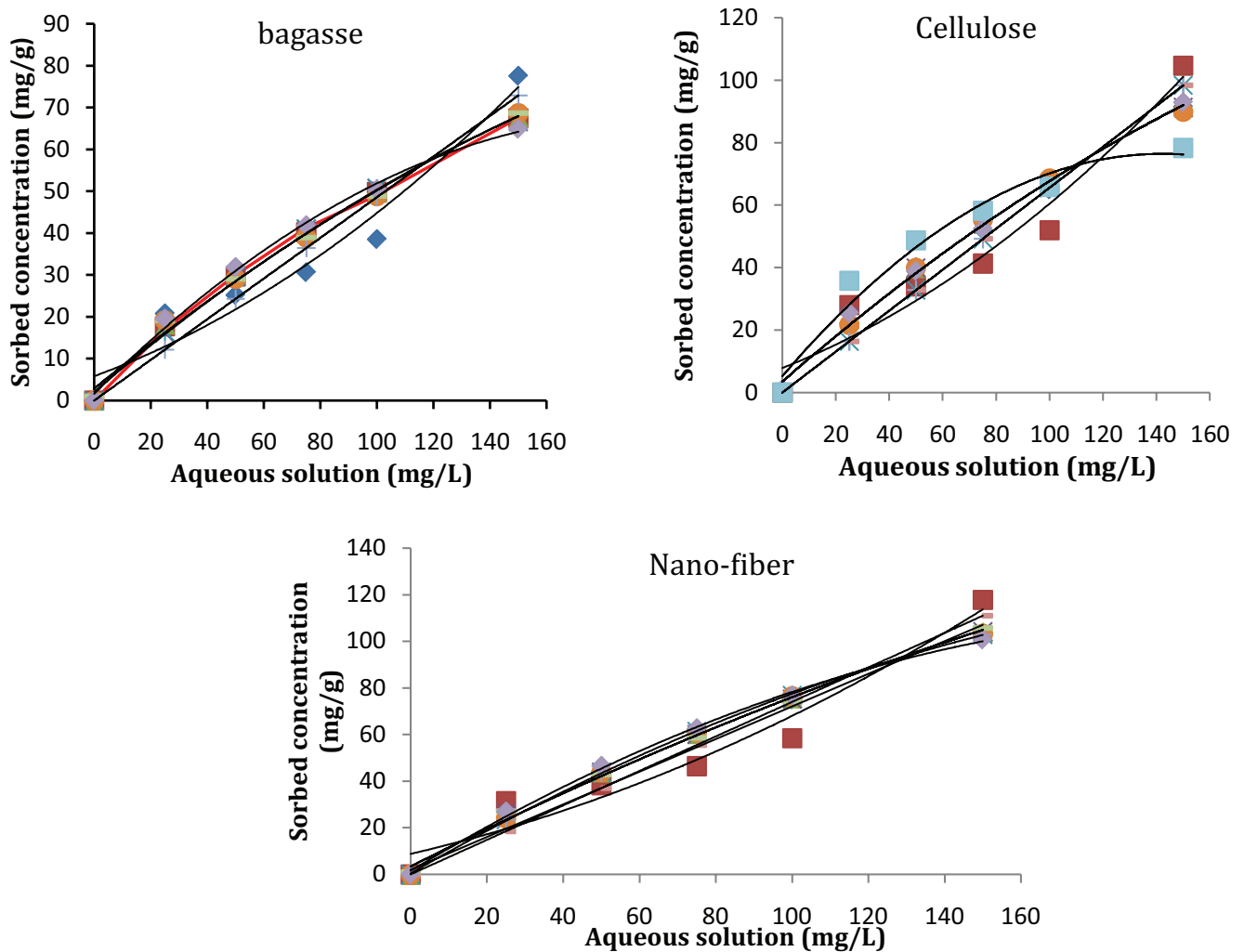


Fig. 13. Plots of fitted isotherms and observed data: Toth, P-P, GLF, linear, Freundlich, Langmuir, F-P, L-P, and BET.

to increase in oxygen evolution and chlorate formation rates. Zhang [66] observed a similar relationship between the current density, treatment time, and regeneration efficiency for the electrochemical regeneration of exhausted activated carbon.

Moreover, the high desorption efficiency at pH 3 is due to the excessive H^+ ions competing for the activated adsorption sites on adsorbents with the MB molecules and replacing the adsorbed MB molecules using ion exchange resulting from desorbing dye molecules from adsorbent. Similar results were observed for desorption of cationic contaminants from aqueous solution on cellulose-based adsorbents [39,67–69]. The results of several consecutive adsorption–desorption cycles are shown in Table 8. It can be seen that the adsorption capacity of MB adsorbed on prepared adsorbents slightly decreased after two cycles of adsorption–desorption process.

To further understand the effect of electrochemical oxidation process on adsorbents regeneration and dye degradation, a gas chromatography-mass spectrometry (GC-MS) analysis was performed to identify the intermediate products in the regeneration solution. As shown in Fig. 15, some organic compounds, such as 1-ethyl-2 methylbenzene,

1,2,3-trimethylbenzene, and 2,4,5-trichlorophenol can be generated in the system. According to these results, it can be concluded that at the regeneration process MB could be desorbed on the surface of the adsorbents, then are oxidized at particle electrodes inside, or oxidized at Ti/TiO_2 - RuO_2 anode directly.

4. Conclusions

In this work, the bleached bagasse and cellulose prepared from bagasse with cellulose nanofiber purchased from Iranian companies have been successfully used as an adsorbing agent for the removal of MB dye from aqueous solutions. Adsorption was influenced by various parameters such as initial pH, initial dye concentration, and dose of adsorbent. The maximum adsorption of MB dye by the three adsorbents occurred at an initial pH of 7. Percent removal of MB dye decreased with increase in initial concentration but increased with increase in adsorbent concentration. The sorption rate of MB on adsorbents was very fast and reaches sorption equilibrium within 60 min. The kinetic parameters were evaluated using the pseudo-first-order, pseudo-second-order, and the Elovich kinetic models.

Table 5
Summary of selected diagnostics for MB adsorbed by bagasse and its derivatives

Adsorbent	Isotherms	AICc	R^2_y	R^2_N	M^2	Linearity assessment
The bleached bagasse	BET	31.40	0.847	0.907	2.6×10^2	Non-linear
	Freundlich	6.28	0.998	0.948	5.8×10^{-1}	Non-linear
	F-P	27.76	0.998	0.983	5.8×10^1	Non-linear
	Langmuir	9.79	0.997	0.746	3.85×10^{-3}	Linear
	L-F	29.0092	0.997	0.749	2.49×10^2	Non-linear
	L-P	34.41	0.992	0.993	4.35×10^2	Non-linear
	Linear	18.71	0.992	0.882	8.87×10^{-1}	Linear
	P-P	14.44	0.992	0.993	3.47×10^{-6}	Linear
Cellulose	Toth	36.66	0.997	0.846	1.02	Non-linear
	BET	34.40	0.844	0.94	2.56×10^2	Non-linear
	Freundlich	15.57	0.994	0.93	2.98	Non-linear
	F-P	36.065	0.994	0.883	8.76×10^1	Non-linear
	Langmuir	21.64	0.987	0.861	3.72×10^{-1}	Linear
	L-F	36.50	0.993	0.794	1.22×10^2	Non-linear
	L-P	21.64	0.987	0.861	7.68×10^{-1}	Linear
	Linear	21.64	0.987	0.861	4.24×10^{-1}	Linear
Nanofiber cellulose	P-P	19.73	0.987	0.94	7.2×10^{-3}	Linear
	Toth	52.33	0.99	0.935	1.26×10^{-1}	Non-linear
	BET	35.57	0.838	0.904	2.59×10^2	Non-linear
	Freundlich	13.23	0.998	0.972	1.27	Non-linear
	F-P	35.24	0.996	0.97	5.53×10^1	Non-linear
	Langmuir	14.33	0.999	0.803	1.61×10^{-3}	Linear
	L-F	30	0.999	0.952	8.21	Non-linear
	L-P	14.33	0.999	0.805	1.614×10^{-3}	Linear
	Linear	21.29	0.990	0.858	4.94×10^{-8}	Linear
	P-P	17.5	0.990	0.974	9.7×10^1	Non-linear
	Toth	38.81	0.999	0.939	1.49	Non-linear

Notes: AICc, multi model ranking; R^2_y , correlation between measured and simulated observation; R^2_N , correlation between residual and normality; M^2 , Linssen measure of non-linearity; L-F, Langmuir-Freundlich.

Table 6
Selected ISOFIT post regression output (Freundlich isotherm)

Parameter or statistic	ISOFIT result			
	Bagasse	Cellulose	Nanofiber	
Overall quality of fit	Weighted sum of squared error	2.37	1.52×10^1	9.55
	Root of mean square error	0.769	1.95	1.54
Parameter statistics	R_y	0.998	0.994	0.998
	K_f	1.6	2.07	2.01
	1/n	0.746	0.755	0.786
Parameter standard error	M^2	0.853	2.98	1.279
	Threshold	0.1	0.1	0.1
Normality (R^2_N)	Assessment	Non-linear	Non-linear	Non-linear
	R^2_N	0.948	0.930	0.972
Runs test	Assessment	Normal residuals	Normal residuals	Normal residuals
	Number of runs	4	4	3
	p-Value	0.90	0.90	0.50
Durbin-Watson test (D)	Assessment	No correlation	No correlation	No correlation
	D	2.47	2.74	1.70
	p-Value	0.589	0.73	0.339
	Assessment	No correlation	No correlation	No correlation

Table 7
Comparison of adsorption capacities of various adsorbents for MB dye

Adsorbents	MB dye concentration, (mg/L)	q_{max} (mg/g)	Isotherm	Kinetic model	Source
Coconut bunch waste	50–500	70.92	Langmuir	Pseudo-second order	[56]
Peanut hull	10–200	68.03	Langmuir	Pseudo-first order	[57]
Walnut sawdust	50–750	59.17	Langmuir	Pseudo-second order	[58]
Rice husk	10–125	40.58	Langmuir	Pseudo-second order	[59]
Hazelnut shells	–	38.22	Langmuir	–	[60]
Carbonized press mud	100–1,000	51.02	Freundlich	Pseudo-second order	[61]
Green alga <i>Ulva lactuca</i>	5–25	40.2	Langmuir Freundlich	Pseudo-second order	[62]
Pyrophyllite	20–150	70.42	Langmuir	Pseudo-second order	[63]
Perlite	–	53.1	Langmuir	–	[64]
Charcoal	0–200	62.7	–	Pseudo-second order	[65]
Olive pomace	0–200	42.3	–	Pseudo-second order	[65]
The bleached bagasse	25–150	73.5	Freundlich	Pseudo-second order	This study
Cellulose	25–150	94.33	Freundlich	Pseudo-second order	This study
Nanofiber cellulose	25–150	119.04	Freundlich	Pseudo-second order	This study

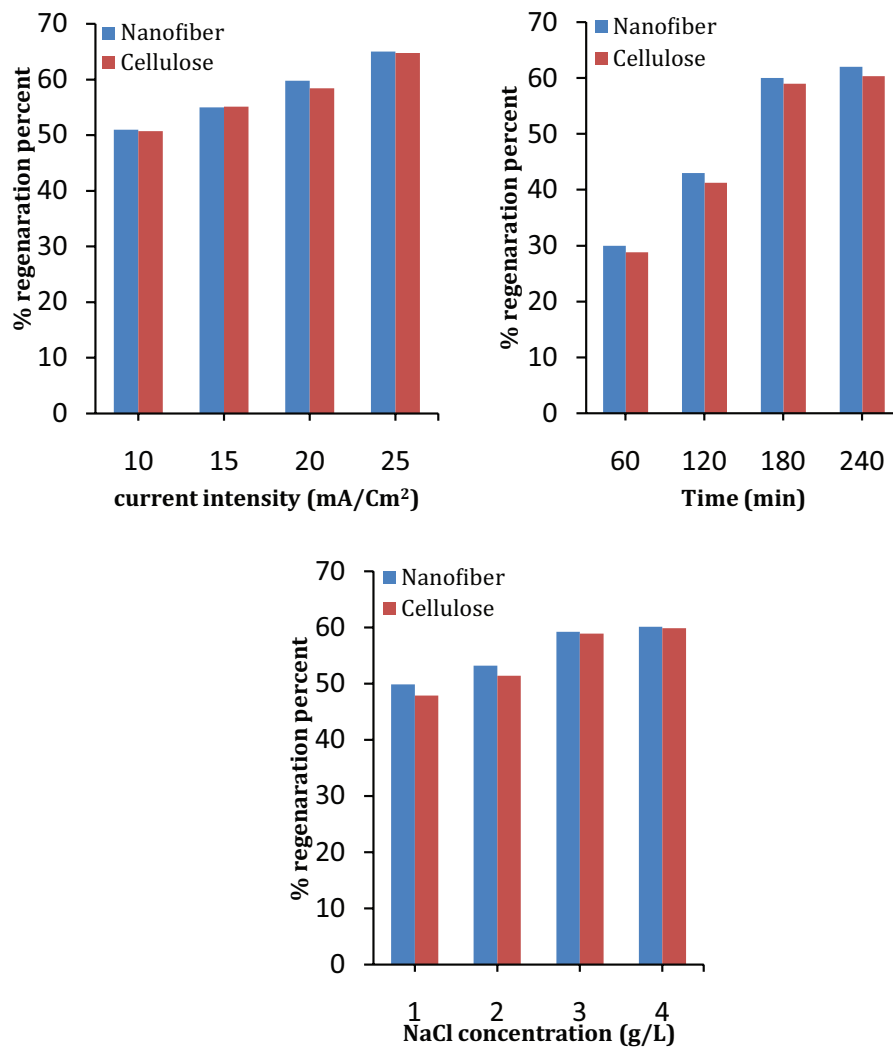


Fig. 14. Impact of various factors on electrochemical regeneration of adsorbents.

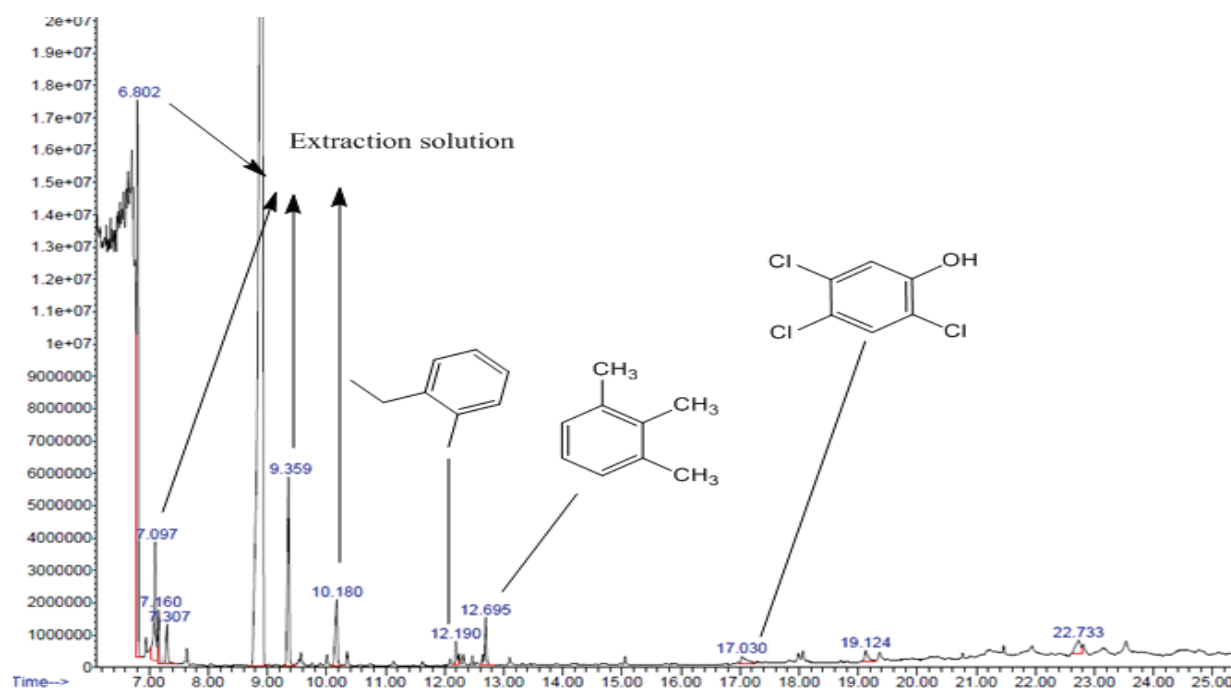


Fig. 15. GC-MS chromatograms of samples taken of electrochemical regeneration of cellulose.

Table 8
Efficiency of adsorbents regeneration

Time	Control	1	2	3
Adsorption capacity of cellulose (mg/g)	91.5	54.90	45.75	27.45
Adsorption capacity of nanofiber cellulose (mg/g)	103.5	62.10	56.925	31.62

The kinetics of the sorption process was found to follow the pseudo-second-order kinetic model. Isotherms study shows that Freundlich isotherm expression provides the best fit for MB sorption by adsorbents.

From the results calculated from Langmuir model, the maximum adsorption capacities of MB on the bleached bagasse, cellulose, and nanofiber cellulose are 73.5, 94.33, and 119.04 mg/g, respectively. The comparison of the results of adsorption capacities of various adsorbents for MB showed that the cellulose nanofiber and cellulose perform better in terms of MB adsorption than many other sorbents. Electrochemical regeneration of studies showed that the regeneration efficiency increased by increasing the regeneration current intensity and regeneration time. The continuous sorption–desorption studies showed that the cellulose and nanofiber cellulose could be regenerated and reused twice. As a result, bagasse and its derivatives can be effectively used for the treatment of wastewater containing MB with cost-effective and reusable properties.

Acknowledgment

We are grateful for the financial support provided by Environmental Health Research Center, Golestan University of Medical Sciences.

References

- [1] N. Kannan, M.M. Sundaram, Kinetics and mechanism of removal of methylene blue by adsorption on various carbons—a comparative study, *Dyes Pigm.*, 51 (2001) 25–40.
- [2] Y. Bulut, H. Aydın, A kinetics and thermodynamics study of methylene blue adsorption on wheat shells, *Desalination*, 194 (2006) 259–267.
- [3] A. Houas, H. Lachheb, M. Ksibi, E. Elaloui, C. Guillard, J.M. Herrmann, Photocatalytic degradation pathway of methylene blue in water, *Appl. Catal., B*, 31 (2001) 145–157.
- [4] B.H. Hameed, A.A. Ahmad, Batch adsorption of methylene blue from aqueous solution by garlic peel, an agricultural waste biomass, *J. Hazard. Mater.*, 164 (2009) 870–875.
- [5] M. Rafatullah, O. Sulaiman, R. Hashim, A. Ahmad, Adsorption of methylene blue on low-cost adsorbents: a review, *J. Hazard. Mater.*, 177 (2010) 70–80.
- [6] S. Yuan, Z. Li, Y. Wang, Effective degradation of methylene blue by a novel electrochemically driven process, *Electrochem. Commun.*, 29 (2013) 48–51.
- [7] A.K. Verma, R.R. Dash, P. Bhunia, A review on chemical coagulation/flocculation technologies for removal of colour from textile wastewaters, *J. Environ. Manage.*, 93 (2012) 154–168.
- [8] N. Zaghbani, A. Hafiane, M. Dhahbi, Separation of methylene blue from aqueous solution by micellar enhanced ultrafiltration, *Sep. Purif. Technol.*, 55 (2007) 117–124.
- [9] T. Zhang, T. Oyama, A. Aoshima, H. Hidaka, J. Zhao, N. Serpone, Photooxidative *N*-demethylation of methylene blue in aqueous TiO₂ dispersions under UV irradiation, *J. Photochem. Photobiol., A*, 140 (2001) 163–172.
- [10] G.L. Dotto, J.M.N. Santos, I.L. Rodrigues, R. Rosa, F.A. Pavan, E.C. Lima, Adsorption of Methylene Blue by ultrasonic surface modified chitin, *J. Colloid Interface Sci.*, 446 (2015) 133–140.
- [11] A. Gürses, Ç. Doğan, M. Yalçın, M. Açıkıldız, R. Bayrak, S. Karaca, The adsorption kinetics of the cationic dye, methylene blue, onto clay, *J. Hazard. Mater.*, 131 (2006) 217–228.
- [12] S. Lin, Z. Song, G. Che, A. Ren, P. Li, C. Liu, J. Zhang, Adsorption behavior of metal–organic frameworks for methylene blue from aqueous solution, *Microporous Mesoporous Mater.*, 193 (2014) 27–34.
- [13] M.S.U. Rehman, I. Kim, J.I. Han, Adsorption of methylene blue dye from aqueous solution by sugar extracted spent rice biomass, *Carbohydr. Polym.*, 90 (2012) 1314–1322.

- [14] Y. Zhang, W. Wang, J. Zhang, P. Liu, A. Wang, A comparative study about adsorption of natural palygorskite for methylene blue, *Chem. Eng. J.*, 262 (2015) 390–398.
- [15] S. Hong, C. Wen, J. He, F. Gan, Y.S. Ho, Adsorption thermodynamics of Methylene Blue onto bentonite, *J. Hazard. Mater.*, 167 (2009) 630–633.
- [16] C.D. Woolard, J. Strong, C.R. Erasmus, Evaluation of the use of modified coal ash as a potential sorbent for organic waste streams, *Appl. Geochem.*, 17 (2002) 1159–1164.
- [17] C.A.P. Almeida, N.A. Debacher, A.J. Downs, L. Cottet, C.A.D. Mello, Removal of methylene blue from colored effluents by adsorption on montmorillonite clay, *J. Colloid Interface Sci.*, 332 (2009) 46–53.
- [18] D.S.P. Franco, J.S. Piccin, E.C. Lima, G.L. Dotto, Interpretations about methylene blue adsorption by surface modified chitin using the statistical physics treatment, *Adsorption*, 21 (2015) 557–564.
- [19] M.H. Hussin, N.A. Pohan, Z.N. Garba, M.J. Kassim, A.A. Rahim, N. Brosse, M. Yemloul, M.N. Fazita, M.M. Haafiz, Physicochemical of microcrystalline cellulose from oil palm fronds as potential methylene blue adsorbents, *Int. J. Biol. Macromol.*, 92 (2016) 11–19.
- [20] X. He, K.B. Male, P. Nesterenko, D. Brabazon, B. Paull, J.H. Luong, Adsorption and desorption of methylene blue on porous carbon monoliths and nanocrystalline cellulose, *ACS Appl. Mater. Interfaces*, 5 (2013) 8796–8804.
- [21] R.R. Krishni, K.Y. Foo, B.H. Hameed, Adsorptive removal of methylene blue using the natural adsorbent-banana leaves, *Desal. Wat. Treat.*, 52 (2014) 6104–6112.
- [22] D. Balarak, J. Jaafari, G. Hassani, Y. Mahdavi, I. Tyagi, S. Agarwal, V.K. Gupta, The use of low-cost adsorbent (Canola residues) for the adsorption of methylene blue from aqueous solution: isotherm, kinetic and thermodynamic studies, *Colloids Interface Sci. Commun.*, 7 (2015) 16–19.
- [23] M. Peydayesh, A. Rahbar-Kelishami, Adsorption of methylene blue onto *Platanus orientalis* leaf powder: kinetic, equilibrium and thermodynamic studies, *J. Ind. Eng. Chem.*, 21 (2015) 1014–1019.
- [24] E.S. Abdel-Halim, Chemical modification of cellulose extracted from sugarcane bagasse: preparation of hydroxyethyl cellulose, *Arabian J. Chem.*, 7 (2014) 362–371.
- [25] A.Mandal, D. Chakrabarty, Isolation of nanocellulose from waste sugarcane bagasse (SCB) and its characterization, *Carbohydr. Polym.*, 86 (2011) 1291–1299.
- [26] W. Chen, H. Yu, Y. Liu, P. Chen, M. Zhang, Y. Hai, Individualization of cellulose nanofibers from wood using high-intensity ultrasonication combined with chemical pretreatments, *Carbohydr. Polym.*, 83 (2011) 1804–1811.
- [27] D. Hu, P. Wang, J. Li, L. Wang, Functionalization of microcrystalline cellulose with *N,N*-dimethyldodecylamine for the removal of Congo Red dye from an aqueous solution, *BioResources*, 9 (2014) 5951–5962.
- [28] F. Bouatay, N. Meksi, F. Slah, F.M. Mohamed, Chemical modification of cellulosic fibers using eco-friendly compounds to improve dyeing with cationic dyes, *J. Text. Sci. Eng.*, 4 (2014) 1.
- [29] I. Shahabi-Ghahfarrokhi, F. Khodaiyan, M. Mousavi, H. Yousefi, Preparation and characterization of nanocellulose from beer industrial residues using acid hydrolysis/ultrasound, *Fibers Polym.*, 16 (2015) 529.
- [30] J.X. Sun, X.F. Sun, H. Zhao, R.C. Sun, Isolation and characterization of cellulose from sugarcane bagasse, *Polym. Degrad. Stab.*, 84 (2004) 331–339.
- [31] H.D. Nguyen, T.T.T. Mai, N.B. Nguyen, T.D. Dang, M.L.P. Le, T.T. Dang, A novel method for preparing microfibrillated cellulose from bamboo fibers, *Adv. Nat. Sci. Nanosci. Nanotechnol.*, 4 (2013) 015016.
- [32] Y. Chen, Q. Wu, B. Huang, M. Huang, X. Ai, Isolation and characteristics of cellulose and nanocellulose from lotus leaf stalk agro-wastes, *BioResources*, 10 (2014) 684–696.
- [33] N.S. Lani, N. Ngadi, A. Johari, M. Jusoh, Isolation, characterization, and application of nanocellulose from oil palm empty fruit bunch fiber as nanocomposites, *J. Nanomater.*, 2014 (2014) 13.
- [34] M. Kosmulski, pH-dependent surface charging and points of zero charge. IV. Update and new approach, *J. Colloid Interface Sci.*, 337 (2009) 439–448.
- [35] S. Zaheer, H.N. Bhatti, S. Sdaf, Y. Safa, M. Zia-ur-Ruhman, Biosorption characteristics of sugarcane bagasse for the removal of foron blue E-BL dye from aqueous solutions, *The J. Animal. Plant Sci.*, 24 (2014) 272–279.
- [36] N. Mohammed, N. Grishewich, R.M. Berry, K.C. Tam, Supplementary information: cellulose nanocrystal–alginate hydrogel beads as novel adsorbents for organic dyes in aqueous solutions, *Cellulose*, 22 (2015), 3725–3738.
- [37] M. Farnane, H. Tounsadi, A. Machrouhi, A. Elhalil, F.Z. Mahjoubi, M. Sadiq, M. Abdennouri, S. Qourzal, N. Barka, Dye removal from aqueous solution by raw maize corncob and H₂PO₄ activated maize corncob, *J. Water Reuse Desal.*, 8 (2018) 214–224.
- [38] L.W. Low, T.T. Teng, M. Rafatullah, N. Morad, B. Azahari, Adsorption studies of methylene blue and malachite green from aqueous solutions by pretreated lignocellulosic materials, *Sep. Sci. Technol.*, 48 (2013), 1688–1698.
- [39] C.H. Chan, C.H. Chia, S. Zakaria, M.S. Sajab, S.X. Chin, Cellulose nanofibrils: a rapid adsorbent for the removal of methylene blue, *RSC Adv.*, 5 (2015) 18204–18212.
- [40] K. Xie, W. Zhao, X. He, Adsorption properties of nano-cellulose hybrid containing polyhedral oligomeric silsesquioxane and removal of reactive dyes from aqueous solution, *Carbohydr. Polym.*, 83 (2011) 1516–1520.
- [41] H. Qiao, Y. Zhou, F. Yu, E. Wang, Y. Min, Q. Huang, L. Pang, T. Ma, Effective removal of cationic dyes using carboxylate-functionalized cellulose nanocrystals, *Chemosphere*, 141 (2015) 297–303.
- [42] R. Batmaz, N. Mohammed, M. Zaman, G. Minhas, R.M. Berry, K.C. Tam, Cellulose nanocrystals as promising adsorbents for the removal of cationic dyes, *Cellulose*, 21 (2014) 1655–1665.
- [43] S.P. Raghuvanshi, R. Singh, C.P. Kaushik, A.K. Raghav, Kinetics study of methylene blue dye bioadsorption on bagasse, *Appl. Ecol. Environ. Res.*, 2 (2004) 35–43.
- [44] A. Kardam, K.R. Raj, S. Srivastava, M.M. Srivastava, Nanocellulose fibers for biosorption of cadmium, nickel, and lead ions from aqueous solution, *Clean Technol. Environ. Policy*, 16 (2014), 385–393.
- [45] S.A. Saad, K.M. Isa, R. Bahari, Chemically modified sugarcane bagasse as a potentially low-cost biosorbent for dye removal, *Desalination*, 264 (2010) 123–128.
- [46] Z. Zhang, I.M. O'Hara, G.A. Kent, W.O. Doherty, Comparative study on adsorption of two cationic dyes by milled sugarcane bagasse, *Ind. Crops Prod.*, 42 (2013) 41–49.
- [47] D. Kavitha, C. Namasivayam, Experimental and kinetic studies on methylene blue adsorption by coir pith carbon, *Bioresour. Technol.*, 98 (2007) 14–21.
- [48] Y. Liu, Y. Kang, B. Mu, A. Wang, Attapulgit/bentonite interactions for methylene blue adsorption characteristics from aqueous solution, *Chem. Eng. J.*, 237 (2014) 403–410.
- [49] F. Kallel, F. Bouaziz, F. Chaari, L. Belghith, R. Ghorbel, S.E. Chaabouni, Interactive effect of garlic straw on the sorption and desorption of Direct Red 80 from aqueous solution, *Process. Saf. Environ. Prot.*, 102 (2016) 30–43.
- [50] H. Cherifi, B. Fatima, H. Salah, Kinetic studies on the adsorption of methylene blue onto vegetal fiber activated carbons, *Appl. Surf. Sci.*, 282 (2013) 52–59.
- [51] T. Liu, Y. Li, Q. Du, J. Sun, Y. Jiao, G. Yang, Z. Wang, Y. Xia, W. Zhang, K. Wang, H. Zhu, Adsorption of methylene blue from aqueous solution by grapheme, *Colloids Surf., B*, 90 (2012) 197–203.
- [52] M. Doğan, Y. Özdemir, M. Alkan, Adsorption kinetics and mechanism of cationic methyl violet and methylene blue dyes onto sepiolite, *Dyes Pigm.*, 75 (2007) 701–713.
- [53] N.O. San Keskin, A. Celebioglu, O.F. Sarioglu, A.D. Ozkan, T. Uyar, T. Tekinay, Removal of a reactive dye and hexavalent chromium by a reusable bacteria attached electrospun nanofibrous web, *RSC Adv.*, 5 (2015) 86867–86874.
- [54] C. Namasivayam, N. Muniasamy, K. Gayatri, M. Rani, K. Ranganathan, Removal of dyes from aqueous solutions by

- cellulosic waste orange peel, *Bioresour. Technol.*, 57 (1996) 37–43.
- [55] H. Nourmoradi, A. Ebrahimi, Y. Hajizadeh, S. Nemati, A. Mohammadi, Application of nano-zeolite and nano-carbon for the removal of humic acid from aqueous solutions, *Int. J. Pharm. Technol.*, 8 (2016) 13337–13352.
- [56] B.H. Hameed, D.K. Mahmoud, A.L. Ahmad, Equilibrium modeling and kinetic studies on the adsorption of basic dye by a low-cost adsorbent: Coconut (*Cocos nucifera*) bunch waste, *J. Hazard. Mater.*, 158 (2008) 65–72.
- [57] R. Gong, M. Li, C. Yang, Y. Sun, J. Chen, Removal of cationic dyes from aqueous solution by adsorption on peanut hull, *J. Hazard. Mater.*, 121 (2005) 247–250.
- [58] F. Ferrero, Dye removal by low cost adsorbents: hazelnut shells in comparison with wood sawdust, *J. Hazard. Mater.*, 142 (2007) 144–152.
- [59] V. Vadivelan, K.V. Kumar, Equilibrium, kinetics, mechanism, and process design for the sorption of methylene blue onto rice husk, *J. Colloid Interface Sci.*, 286 (2005) 90–100.
- [60] M. Doğan, H. Abak, M. Alkan, Biosorption of methylene blue from aqueous solutions by hazelnut shells: equilibrium, parameters and isotherms, *Water Air Soil Pollut.*, 192 (2008) 141–153.
- [61] C. Duran, D. Ozdes, A. Gundogdu, H.B. Senturk, Kinetics and isotherm analysis of basic dyes adsorption onto almond shell (*Prunus dulcis*) as a low cost adsorbent, *J. Chem. Eng. Data*, 56 (2011) 2136–2147.
- [62] A. El Sikaily, A. Khaled, A.E. Nemr, O. Abdelwahab, Removal of methylene blue from aqueous solution by marine green alga *Ulva lactuca*, *Chem. Ecol.*, 22 (2006) 149–157.
- [63] A. Gücek, S. Şener, S. Bilgen, M.A. Mazmançı, Adsorption and kinetic studies of cationic and anionic dyes on pyrophyllite from aqueous solutions, *J. Colloid Interface Sci.*, 286 (2005) 53–60.
- [64] M. Doğan, M. Alkan, Y. Onganer, Adsorption of methylene blue from aqueous solution onto perlite, *Water Air Soil Pollut.*, 120 (2000) 229–248.
- [65] F. Banat, S. Al-Asheh, R. Al-Ahmad, F. Bni-Khalid, Bench-scale and packed bed sorption of methylene blue using treated olive pomace and charcoal, *Bioresour. Technol.*, 98 (2007) 3017–3025.
- [66] H. Zhang, Regeneration of exhausted activated carbon by electrochemical method, *Chem. Eng. J.*, 85 (2002) 81–85.
- [67] X. Li, Y. Tang, Z. Xuan, Y. Liu, F. Luo, Study on the preparation of orange peel cellulose adsorbents and biosorption of Cd²⁺ from aqueous solution, *Sep. Purif. Technol.*, 55 (2007) 69–75.
- [68] D. Zhou, L. Zhang, J. Zhou, S. Guo, Cellulose/chitin beads for adsorption of heavy metals in aqueous solution, *Water Res.*, 38 (2004) 2643–2650.
- [69] D.W. O'Connell, C. Birkinshaw, T.F. O'Dwyer, A modified cellulose adsorbent for the removal of nickel (II) from aqueous solutions, *J. Chem. Technol. Biotechnol.*, 81 (2006) 1820–1828.